REVISTA MATÉRIA V.22 N.02
ISSN 1517-7076 artigo e11813, 2017

Microstructure and hardness of cement pastes with mineral admixture

Dayana Cristina Silva Garcia[1], Marcela Maira Nascimento de Souza Soares[2], Augusto Cesar da Silva Bezerra[3], Maria Teresa Paulino Aguilar[4], Roberto Braga Figueiredo[5]

[1] Department of Metallurgical Engineering, Universidade Federal de Minas Gerais CEP: 31270-901, Belo Horizonte, MG. e-mail: dayanacsgarcia@yahoo.com.br
[2] Department of Mining Engineering and Civil Construction, Centro Federal de Educação Tecnológica de Minas Gerais CEP: 38180-510, Araxá ,MG. e-mail: mmaira_br@yahoo.com.br
[3]Department of Materials Engineering, Centro Federal Tecnológico de Minas Gerais CEP: 30421-169, Belo Horizonte, MG. e-mail: augustobezerra@des.cefetmg.br
[4]Department of Materials Engineering and Civil Construction, Universidade Federal de Minas Gerais CEP: 31270-901, Belo Horizonte, MG. e-mail: teresa@ufmg.br
[5]Department of Materials Engineering and Civil Construction, Universidade Federal de Minas Gerais CEP: 31270-901, Belo Horizonte, MG. e-mail: figueiredo@demc.ufmg.br

ABSTRACT

Portland cement pastes are highly heterogeneous material and exhibits heterogeneous features over a wide range of length scales. Mechanical properties of microstructure can be determined using depth-sensing indentation. Coupled indentation/SEM technique can be used to location the indents and provides a way to determine the mechanical properties of a specific phase. Thus, the present paper aims to determine the hardness of different phases of cement pastes prepared with different mineral admixtures including sugarcane bagasse ash. The microstructure of cement pastes prepared with different mineral admixtures is analyzed by X ray diffraction, scanning electron microscopy and dynamic hardness tests on polished sections. The different backscatter coefficient allows to differentiate anhydrous phases from C-S-H, calcium hydroxide, silica fume and quartz. A grid of indentation is used to determine the hardness of the different phases and a complete phase segmentation of the different samples is achieved. The results show that the hardness of the different phases follow the sequence (from higher to lower hardness) quartz, anhydrous particles, calcium hydroxide, C-S-H and agglomerated silica fume. The presence of agglomerated silica fume is clearly observed in scanning electron microscopy images and the poor mechanical properties of these areas might compromise the cement pastes. The microstructure of cement pastes prepared with sugarcane bagasse ashes is similar to the observed in samples with crushed quartz.

Keywords: Dynamic hardness, cement paste, sugarcane bagasse ash, silica fume, scanning electron microscopy.

1. INTRODUCTION

Cement pastes are highly heterogeneous materials due to the multiple constituent phases and multiple processing conditions. Microstructure and general properties of the composite depend on the source materials, mixture proportions, conditions of curing and rate of hydration. Thus, understanding the microstructure of cement pastes is important to understand the effect of processing conditions. Images of Portland cement pastes by scanning electron microscopy (SEM) have showed that pore structure is influence by the type of binder, curing time and the water/binder ratio[1]. Also, SEM shows that the microstructure is complex and contains different phases [2,3]. Thus, backscattered electrons SEM images have been used to differentiate phases within hydrated cement pastes. For example, it is possible to separate particles of calcium hydroxide, residual unhydrated cement grains, C-S-H and pores [4,5].

Furthermore, the Portland cement pastes exhibits heterogeneous features over a wide range of length scales and it is known that compression strength, hardness, permeability and durability of cement-based materials are dependent of properties of nano/microscale [6-8]. The investigation of the micromechanical properties of cementitious materials has been used to determine the properties of different constituents of Portland

Autor Responsável: Dayana Cristina Silva Garcia Data de envio: 18/04/2016 Data de aceite: 23/09/2016

10.1590/S1517-707620170002.0145

cement pastes. Some papers have used the depth-sensing indentation to study the mechanical properties of various cementitious materials [9-13].

The coupled indentation/SEM technique allows the interpretation of mechanical properties of Portland cement paste using the micromechanical properties of specific areas. The SEM can be used to location the indents and provides a way to determine the mechanical properties of a specific phase [14,15] and the arrangement of the phases of cement paste [16,17]. It is known that the hardness of pure anhydrous materials is higher than their hydrated counterparts [18-20].

Nowadays, mineral admixtures like silica fume and sugarcane bagasse ash (SCBA) have been used to replace Portland cement. These materials improve the mechanical performance and durability of Portland cement pastes through microstructure control due to pozzolanic reactions that reduces permeability and chloride ion diffusion [21-23]. It is known that SCBA contains quartz but there are reports in the literature that this material exhibits pozzolanic activity[23-27]. Some works have been conducted to study the properties of C-S-H, Portland cement phases and pastes prepared with materials pozzolanic materials [28-30]. However, the hardness of different phases in Portland cement pastes incorporating sugarcane bagasse ash has not been reported. The understanding of the effect of sugarcane bagasse ash on the microstructure and hardness of cement pastes is of particular importance due to the interest in incorporating this residue in cement composites. Thus, the present paper aims to determine the hardness of different phases of cement pastes prepared with different mineral admixtures including sugarcane bagasse ash. Also, the microstructure of the different cement pastes was analyzed with scanning electron microscopy to determine the distribution of phases.

2. MATERIALS AND METHODS

The materials used in the present investigation were ordinary Portland cement (CP-I), silica fume (SF), sugarcane bagasse ash (SCBA) and crushed quartz. The SCBA was collected by Usina Caeté in Delta city, in the State of Minas Gerais, Brazil. The sugarcane bagasse ash was obtained after the bagasse was burned in cogeneration boiler, dried at 60°C for 5 days, milled for 10 hours in a rotary ball mill and further burned in laboratory at 600°C for 4 hours. The chemical compositions of materials determined by energy dispersive X-ray fluorescence are presented in Table 1. The phase constituents of the Portland cement was determined by Bogue calculation as 64.6% of C_3S, 7.6% of C_2S, 6.8% of C_4A and 9.3% of C_4AF. The silica fume (SF) and crushed quartz are composed basically by SiO_2. X-ray diffraction pattern of materials used in this investigation are reported elsewhere [31]. Basically they revealed no crystalline structure for silica fume, peaks of quartz for crushed quartz and peaks associated with C_3S and C_2S for ordinary Portland cement. The SCBA exhibits peaks of quartz showing that at least part of this material has a crystalline structure. Distribution of particle diameters was determined using a CILAS 1064 laser granulometer and results were reported in Figure 1. The results showed average diameter of ~12.2 µm for silica fume, ~4.3 µm for SCBA and ~17.5 µm for quartz.

Table 1: Chemical composition (in wt. %) of the ordinary Portland cement (OPC) and the sugarcane bagasse ash (SCBA).

	SiO_2	Al_2O_3	Fe_2O_3	CaO	MgO	TiO_2	P_2O_5	Al	Fe	K	Ti	LOI
OPC	19.6	4.77	3.05	61.4	2.23	0.25	0.12	0.32	0.96	0.1	5.38	5.38
SCBA	72.3	5.52	10.8	1.57	1.13	3.68	1.11	-	-	-	-	1.52

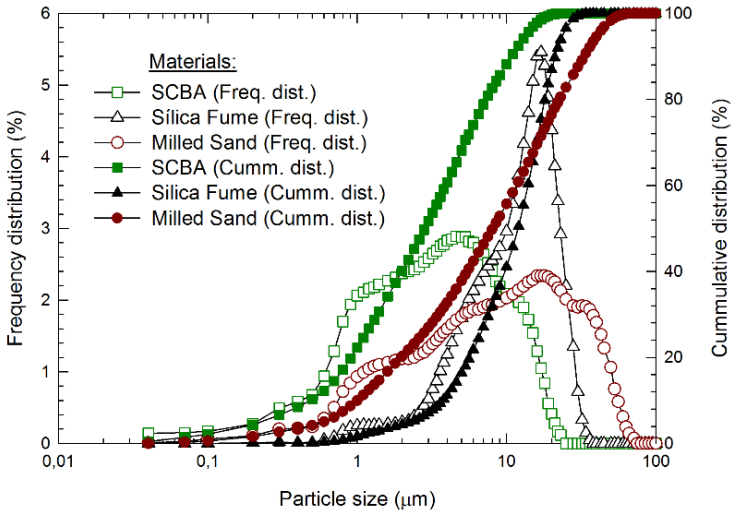

Figure 1: Cumulative and frequency distribution as a function of particle size for the SCBA,

Cement pastes were molded in plastic containers closed with lids. The water/binder ratio used was 0.4 and samples were allowed to moist-cure for 30 days at 60ºC [32]. It has been shown that curing at high temperature accelerates pozzolanic reaction [33]. A reference paste was prepared by mixing only cement and water. Other pastes were prepared with partial substitution of cement by siliceous material (silica fume, ground quartz, and SCBA). The amounts of replacement in each sample were: 5% and 20% of silica fume, 20% of quartz and 20% of SCBA.

After curing the samples were cut using a low speed diamond saw and embedded in acrylic resin. The surfaces were ground and polished with silicon carbide papers (#220, #400, #600, #1200, #2500 and #4000) and the final polishing step was with alumina suspension (1.0 μm). Scanning electron microscopy (SEM) was used to analyze the microstructure. The SEM investigation was carried out on a Hitachi TM-3000 microscope in backscattered electron mode at accelerating voltage of 15 kV, magnification of 250x, with an emission current of 26800 nA and working distance of 6 mm. The images were processed using ImageJ software. The threshold was fixed on the valleys of grey level histogram. The procedure adopted for image processing was based on the literature[3,34,35].

Dynamic hardness tests were carried out using a Shimadzu DUH-211 ultra-microhardness tester operating with load-unloading cycles with loading rate of 5.0 mN/s, Berkovich indenter and maximum load of 100 mN. A grid with 5×5 indentations was used and the area was observed on SEM. The marks were 50 μm apart, in five rows of 5 indents, covering an area of 200x200 μm² on the surface of the samples. The area around each indent was observed on SEM in order to determine the corresponding phase of cement paste. Indentations performed on the interface between different phases were not considered.

X ray diffraction pattern were recorded with a Philips PW1710 diffractometer, using Cu Kα radiation and graphite monochromatic crystal with wavelength $\lambda_1 = 1.5406$ Å.

3. RESULTS

Figure 2 shows the morphology of silica fume, SCBA and quartz. It is observed that silica fume particles are rounded and with very fine particle size. This observation disagrees with the average particle size determined by laser granulometry which is explained by agglomeration of silica fume during measurements. The SCBA exhibits particles similar in size and shape to the quartz but the distribution of particle sizes seems to be more heterogeneous and very fine particles are also observed. Quartz particles are prismatic with sharp edges

Figure 3 shows the X ray diffraction patterns of the different cement pastes. The peaks at $2\Theta \approx 18º$ and 34º are observed in all samples and are associated with calcium hydroxide. However, the intensity of these peaks decrease on pastes prepared with silica fume and SCBA suggesting the occurrence of pozzolanic activity. The quartz peaks are observed on samples prepared with quartz and SCBA.

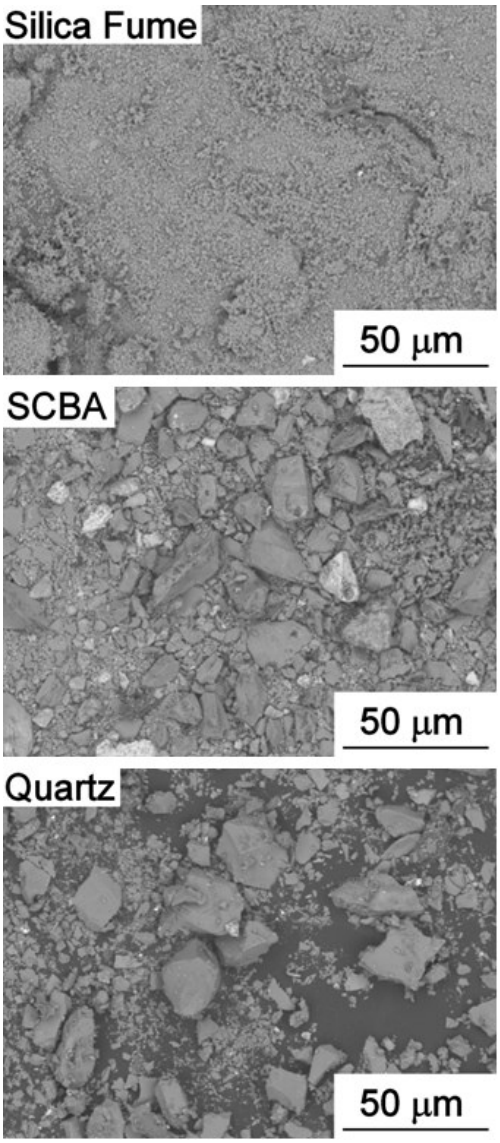

Figure 2: Morphology of the mineral admixture (silica fume, SCBA and quartz) used as partial replacement to cement in pastes.

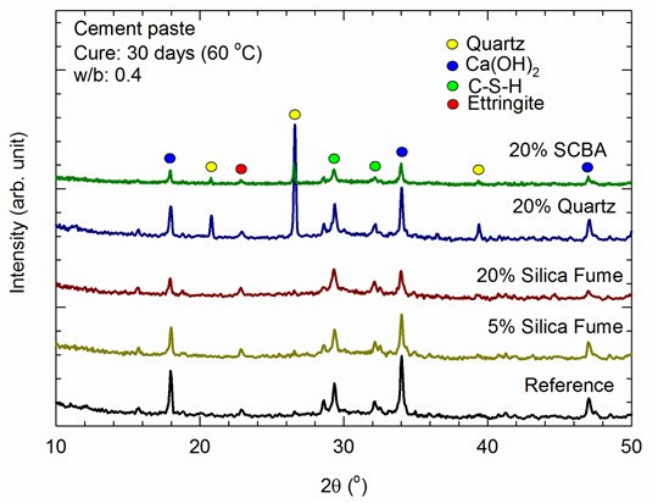

Figure 3: X ray diffraction pattern of reference cement paste and pastes prepared with partial replacement by different mineral admixtures.

Figure 4 shows the grey level histogram (top) and the microstructure (bottom) of a representative area of the cement paste prepared with 20% replacement by silica fume. The gray level histogram presents only two distinct peaks: one small at high brightness and one larger at intermediate gray level. The small peak at high brightness is associated with anhydrous cement phase. Pores are usually associated with low gray (dark) values. However, different phases (C-S-H, CH, S.F., quartz) are associated with intermediate gray levels. The microstructure image shows areas of residual Portland cement (bright phase) and hydrated phases. The microstructure shows a large continuous phase at the bottom-left region and a similar phase at the top-right region. The gray level in these areas is similar to the hydrated phase but the indentations produce larger marks in the former. This shows that these phases exhibit low hardness compared to the hydrated phase and this is attributed to agglomerated silica fume.

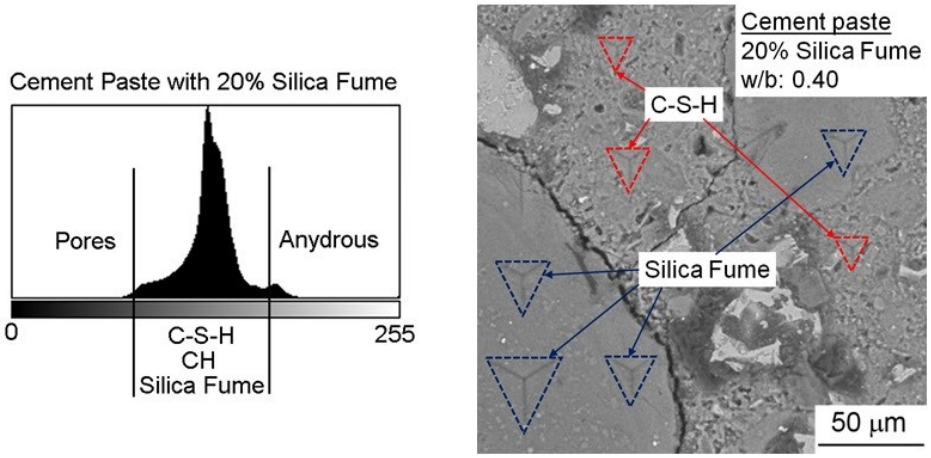

Figure 4: Backscattered electron (BSE) grey level histogram and image of sample prepared with 20% of silica fume as cement replacement

Coupling SEM image and dynamic hardness was adopted for representative areas in the different samples in order to determine the distribution of phases and the hardness of each phase. Figure 5 shows representative curves of dynamic hardness tests at different phases. It is observed that quartz and anhydrous cement phase are associated with the smaller depth of indentation due to the higher hardness of these phases. Calcium hydroxide (CH) also exhibits high hardness followed by C-S-H. The hardness associated with silica fume is the smaller. The low hardness of the silica fume is due to the lack of adhesion between the small particles in agglomerated areas.

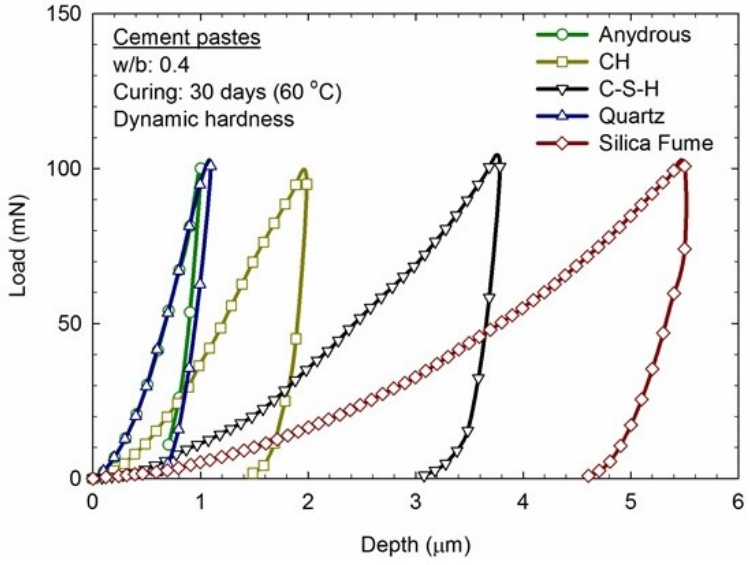

Figure 5: Representative load-depth curves for different phases observed in cement pastes prepared with different mineral admixture.

Table 2 shows a summary of the average hardness for each phase. Quartz exhibits the higher hardness, followed by anhydrous particles, calcium hydroxide, C-S-H and the lowest hardness is observed in agglomerated silica fume. The values of elastic modulus (E) for each phase is also shown and follows a similar trend than observed in hardness, except for the higher elastic modulus of anhydrous phase compared to quartz. The values of hardness for the C-S-H varied slightly depending on the sample constituents. The lowest value (0.27 GPa) was observed in the reference sample and the sample with 20% of quartz and the highest value (0.37 GPa) was observed in the sample with 5% of silica fume. The hardness of the C-S-H of the sample prepared with 20% cement replacement by SCBA is similar than the reference sample and the sample with 20% quartz but lower than the samples with 5% of silica fume. This suggests that SCBA exhibits intermediate behavior between pure quartz and silica fume in the development of hardness of cement pastes hydrated products.

Table 2: Summary of hardness for the different phases observed in cement pastes with different mineral admixture.

Phase	H (GPa)	E (GPa)
Quartz	3.01	43.5
Anhydrous	2.93	68.8
CH	0.92	27.0
C-S-H (Reference)	0.27	18.2
C-S-H (5% Silica Fume)	0.37	18.3
C-S-H (20% Silica Fume)	0.31	18.5
C-S-H (20% Quartz)	0.27	17.0
C-S-H (20% SCBA)	0.30	17.2
Silica fume	0.14	8.1

Although the backscatter coefficients of silica fume, quartz and C-S-H are similar, these phases can be distinguished by their shape and hardness. Thus, the distribution of the phases in the different pastes was determined and Figure 6 shows both the SEM image and the corresponding image segmentation. All samples contain anhydrous phases and calcium hydroxide. Quartz particles were visible on samples with crushed quartz and SCBA. Furthermore, agglomerated silica fume was observed on cement paste with 20% cement replacement by silica fume.

4. DISCUSSION

Many reports in the literature use gray level histograms to differentiate phases in cement pastes. Three peaks are usually observed in these histograms and they are associated with C-S-H, CH and anhydrous phases[2,3,37]. However, the histograms obtained in the present work exhibits only two peaks which are associated with the C-S-H and anhydrous phases. This difference is attributed to the magnification used (250x) in the present experiments. It has been reported that low magnification can prevent the dissociation of the peak of CH[39]. However, the shape of calcium hydroxide phase and its hardness differs from the C-S-H. Quartz and silica fume also exhibit similar gray level to C-S-H. Thus, hardness and phase morphology are used to differentiate these phases. Agglomeration of silica fume took place in the sample prepared with 20% of this constituent which can compromise pozzolanic reactions. Agglomeration of silica fume has been reported in the literature[38].

The present results show that anhydrous cement particles have the highest hardness while C-S-H and silica fume have the lowest. This is in agreement with the literature where the lower hardness was reported in C-S-H[19,20]. Also, a high value of hardness was also observed in quartz [36] which is in agreement with the present investigation. The low hardness observed in agglomerated silica fume in the present experiments shows that the particles are loose. Thus, volumes of unreacted silica fume can compromise the mechanical properties of cement pastes. The values found in the present paper are lower than the hardness observed in work of Hi and Li [18]. According to them, the hardness of anhydrous particles and outer C-S-H were about 8.91 GPa and 0.75, respectively. This difference is attributed to the higher load used for identation in the present experiments.

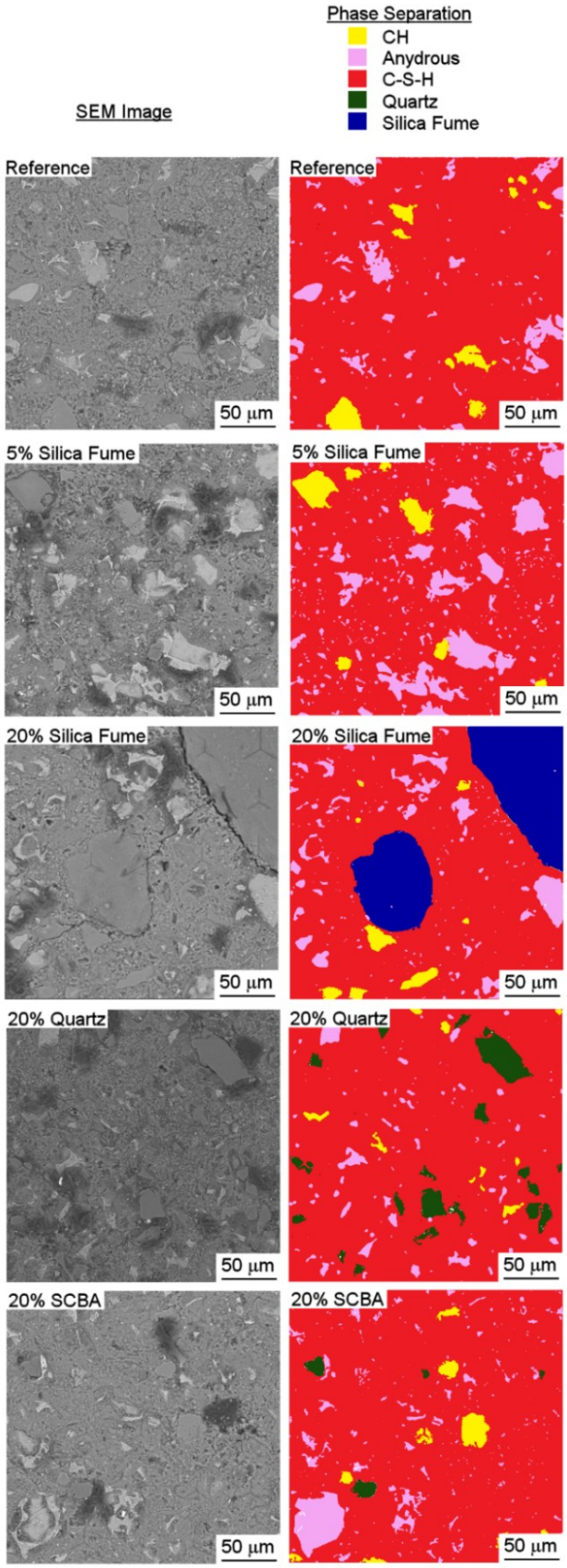

Figure 6: Backscattered electron (BSE) image and phase segmentation of a reference cement paste and pastes prepared with 5% silica fume, 20% silica fume, 20% quartz and 20% sugarcane bagasse ash as cement replacement.

Moreover, the hardness of the C-S-H phase varied in the samples with different mineral admixtures. It was found that the addition of quartz does not affect the hardness of the C-S-H compared to a sample without any mineral admixture. However, the addition of silica fume increases the hardness of this phase and this effect is more pronounced when only 5% of the OPC is replaced compared to the sample with 20% replacement. It was noted that the addition of SCBA leads to an increase of hardness of the C-S-H although this effect was less pronounced compared to the effect of silica fume. The increase in hardness might be attributed to a decrease in porosity although this effect needs further investigation. Thus, sugarcane bagasse ashes exhibits behavior in-between quartz and silica fume on the development of hardness of C-S-H when used as mineral admixture. This observation is in agreement with a recent paper that showed that SCBA exhibits behavior in-between silica fume and quartz on pozzolanic activity [32].

5. SUMMARY AND CONCLUSIONS

- Cement pastes were prepared with addition of quartz, silica fume and sugarcane bagasse ashes. Scanning electron microscopy coupled with dynamic hardness tests were used to analyze the microstructure.
- X ray diffraction revealed the presence of calcium hydroxide in all conditions tested and revealed the presence of quartz in the sample prepared with sugarcane bagasse ashes.
- The histogram of gray level obtained from the SEM images allowed to differentiate the presence of anhydrous phases but does not allow to separate C-S-H, CH, silica fume and quartz.
- The microstructure of samples prepared with 20% of silica fume showed areas of agglomerated silica fume which exhibits low values of hardness.
- The samples prepared with SCBA present microstructure similar to the samples with crushed quartz and the hardness of the C-S-H phase is in-between the sample with quartz and the sample with silica fume.

6. ACKNOWLEDGEMENTS

The authors acknowledge the support from FAPEMIG, CNPq, CAPES and the Graduate Programs in Civil Construction (PPGCC) and in Metallurgical and Materials Engineering (PPGEM) of the Universidade Federal de Minas Gerais.

7. BIBLIOGRAPHY

[1] OUELLET, S., BUSSIÈRE, B., AUBERTIN, M., "Characterization of Cemented Paste Backfill Pore Structure Using SEM and IA Analysis", *Bulletin of Engineering Geology and the Environment*, v. 67, n. 2, pp. 139-152, 2008.

[2] SCRIVENER, K.L., PRATT, P.L., "Backscattered Electron Images of Polished Cement Section in the Scanning Electron Microscope", In: *Proceedings 6th Annual International Conference on Cement Microscopy,* pp. 145-155, Albuquerque, 1984.

[3] KJELLSEN, K.O., DETWILER, R.J., GJORV, O.E., "Backscattered Electron Imaging of Cement Pastes Hydrated at Different Temperatures", *Cement and Concrete Resarch*, v. 20, pp. 308-311, 1990.

[4] DIAMOND, S., "Considerations in Image Analysis as Applied to Investigation of the ITZ in Concrete", *Cement and Concrete Composite,* v. 23, n. 2, pp. 171-178, 2001.

[5] DIAMOND, S., "The Microstructure of Cement Paste and Concrete: a visual primer", *Cement and Concrete Composite,* v. 26, n. 8, pp. 919-933, 2004.

[6] CONSTANTINIDES, G., ULM, F-J., VAN, V.K., "On the use of nanoindentation for cementitious materials", *Materials and Structures*, v. 36, n. 3, pp. 191-196, 2003.

[7] POURBEIK, P., BEAUDOIN, J.J., ALIZADEH, R., *et al*., "Dynamic mechanical thermo-analysis of Portland cement paste hydrated for 45 years", *Materials and Structure,* v. 43, n. 3, pp. 329-340, 2016.

[8] POURBEIK, P., BEAUDOIN, J.J., ALIZADEH, R., *et al.*, "Correlation between dynamic mechanical thermo-analysis and composition-based models for C-S-H in hydrated Portland cement paste", *Materials and Structures,* v. 48, n. 8, pp. 2447-2454, 2015.

[9] IGARASHI, S.B.A., BENTUR, A., MINDESS, S., "Microhardness testing of cementitious materials", *Advanced Cement Based Material,* v. 4, n. 2, pp. 48-57, 1996.

[10] CONSTANTINIDES G, ULM F-J. The effect of two types of C-S-H on the elasticity of cement-based materials: Results from nanoindentation and micromechanical modeling, *Cement and Concrete Resarch.* 2004; 34: 67-80.

[11] MONDAL P, SHAH SP, MARKS L. A reliable technique to determine the local mechanical properties at the nanoscale for cementitious materials. *Cement and Concrete Resarch.* 2007; 37: 1440-1444.

[12] VELEZ, K., MAXIMILIEN, S., DAMIDOT, D., *et al.*, "Determination by nanoindentation of elastic modulus and hardness of pure constituents of Portland cement clinker", *Cement and Concrete Resarch,* v. 31, n. 4, pp. 555-561, 2001.

[13] VANDAMME, M., ULM, F-J., "Nanoindentation investigation of creep properties of calcium silicate hydrates", *Cement and Concrete Resarch*, v. 52, pp. 38-52, 2013.

[14] CHEN, J., SORELLI, L., VANDAMME, M., *et al.*, "A Coupled nanoindentation/SEM-EDS study on low water/cement ratio Portland cement paste: evidence for C–S–H/$Ca(OH)_2$ nanocomposites", *Journal of the American Ceramic Society*, v. 93, n. 5, pp. 1484-1493, 2010.

[15] CONSTANTINIDES, G., ULM, F-J., "The nanogranular nature of C–S–H", *Journal of the Mechanics and Physics of Solids*, v. 55, n. 1, pp. 64-90, 2007.

[16] CONSTANTINIDES, G., CHANDRAN, K.S.R., ULM, F-J., *et al.*, "Grid indentation analysis of composite microstructure and mechanics: principles and validation", *Materials Science and Engineering: A.* v. 430, n. 1, pp. 189-202, 2006.

[17] KRAKOWIAK, K.J., WILSON, W., JAMES, S., *et al*,. "Inference of the phase-to-mechanical property link via coupled X-ray spectrometry and indentation analysis: Application to cement-based materials", *Cement and Concrete Resarch,* v. 67, pp. 271-285, 2015.

[18] HU, C., LI, Z., "Micromechanical investigation of Portland cement paste", *Construction and Building Materials*, v. 71, pp. 44-52, 2004.

[19] ZHU, W., HUGHES, J.J., BICANIC, N., *et al*., "Nanoindentation mapping of mechanical properties of cement paste and natural rocks", *Materials Characterization,* v. 58, n. 11, pp. 1189-1198, 2007.

[20] HUGHES, J.J., TRTIK. P., "Micro-mechanical properties of cement paste measured by depth-sensing nanoindentation: a preliminary correlation of physical properties with phase type", *Materials Characterization*, v. 53, n. 2, pp. 223-231, 2004.

[21] BENTZ, D.P., JENSEN, O.M., COATS, A.M., *et al*., "Influence of silica fume on diffusivity in cement-based materials I. Experimental and computer modeling studies on cement pastes", *Cement and Concrete Resarch,* v. 30, n. 6, pp. 953-962, 2000.

[22] YANG, C.C., CHIANG, C.T., "On the relationship between pore structure and charge passed from RCPT in mineral-free cement-based materials", *Materials chemistry and physics*, v. 93, n. 1, pp. 202-207, 2005.

[23] HUSSEIN, A.A.E., *et al*. "Compressive Strength and Microstructure of Sugar Cane Bagasse Ash Concrete", *Research Journal of Applied Sciences, Engineering and Technology*, v. 7, n. 12, p. 2569-2577, 2014.

[24] RIBEIRO, D.V., MORELLI, M.R., "Effect of calcination temperature on the pozzolanic activity of brasilian sugar cane bagasse ash (SCBA)", Materials Research, v. 17, n. 10, pp. 974-981, 2014.

[25] CORDEIRO, G.C., TOLEDO FILHO, R.D., TAVARES, L.M., *et al*., "Ultrafine grinding of sugar cane bagasse ash for application as pozzolanic admixture in concrete", Cement and Concrete Resarch, v. 39, n.2 , pp. 110-115, 2009.

[26] CORDEIRO, G.C., TOLEDO FILHO, R.D., TAVARES, L.M., *et al*., "Effect of calcination temperature on the pozzolanic activity of sugar cane bagasse ash", *Construction and Building Materals*, v. 23, n. 10, pp.3301-3303, 2009.

[27] FRÍAS, M., VILLAR-COCIÑA, E., "Influence of calcining temperature on the activation of sugar-cane bagasse: Kinetic parameters", *Advances in Cement Research*, v. 19, n.3, pp. 109-115, 2007.

[28] HU, C., "Microstructure and mechanical properties of fly ash blended cement pastes", *Construction and Building Materials*, v. 73, pp. 618-625, 2004.

[29] MONDAL, P., SHAH, S. P., MARKS, L. D., *et al*., "Comparative Study of the Effects of Microsilica and Nanosilica in Concrete", *Transportation research record: journal of the transportation research board*, n. 2141, pp. 6-9, 2010.

[30] TEMIZ, H., KARAKEÇI, A. Y. "Na investigation on microstructure of cement paste containing fly ash and sílica fume", *Cement and Concrete Research*, v. 32, pp. 1131-1132, 2002.

[31] SOARES, M.N.S., FIGUEIREDO, R.B.F., AGUILAR, M.T.P., CETLIN P.R. "Evaluation of pozzolanic activity of siliceous materials using the method of variation of conductivity in lime solution", *Material Science Forum*, pp. 363-368, 2014.

[32] SOARES, M.M.N., GARCIA, D.C.S., FIGUEIREDO, R.B., AGUILAR, M.T.P., CETLIN, P.R., "Comparing the pozzolanic behavior of sugar cane bagasse ash to amorphous and crystalline SiO2", *Cement and Concrete Composites*, v. 71, pp. 20-25, 2016.

[33] ESCALANTE-GARCIA., J. I., SHARP, J., H., "The microstructure and mechanical properties of blended cements hydrated at various temperatures", *Cement and Concrete Research*, v. 31, n. 5, pp. 695-702, 2001.

[34] SULTZMAN, P., "Scanning Electron Microscopy Imaging of Hydraulic Cement Microstructure", *Cement and Concrete Composites*, v. 26, pp. 957-966, 2004.

[35] SCRIVENER, K.L., "Backscattered Electron Imaging of Cementitious Microstructures: understanding and quantification", *Cement and Concrete Composites*, v. 26, pp. 935-945, 2004.

[36] ZHAO, H., DARWIN, D., "Quantitative backscattered electron analysis of cement paste", *Cement and Concrete Resarch*, v. 22, pp.695-706, 1992.

[37] FENG, S., WANG, P., LIU, X., "SEM-backscattered electron imaging and image processing for evaluation of unhydrated cement volume fraction in slag blended Portland cement pastes" *Journal of Wuhan University of Technology-Material. Science. Ed,* v. 28, pp. 968-972, 2013.

[38] DIAMOND, S., SAHU, S., THAULOW, N., "Reaction products of densified silica fume agglomerates in concrete", *Cement and Concrete Research*, v. 31, pp. 1625-1632, 2004.

[39] SORELLI, L., CONSTANTINIDES, G., ULM, F-J., TOUTLEMONDE, F., "The nano-mechanical signature of ultra high performance concrete by statistical nanoindentation techniques", *Cement and Concrete Resarch,* v. 38, pp. 1447-1456, 2008.